Characteristics of a Source for Oxide Coating Deposition by the Electron-Beam Evaporation of Dielectric Materials

Viktor Burdovitsin [1], Ilya Bakeev [1,*], Kirill Karpov [1], Lionel Ngon A. Kiki [1], Efim Oks [1,2] and Alexey Vizir [2]

1. Laboratory of Plasma Electronics, Tomsk State University of Control Systems and Radioelectronics, 634050 Tomsk, Russia; burdovitsin@hotmail.com (V.B.); kkarpov99@gmail.com (K.K.); burdov@fet.tusur.ru (L.N.A.K.); oks@fet.tusur.ru (E.O.)
2. Institute of High-Current Electronics, Siberian Branch of the Russian Academy of Science, 634055 Tomsk, Russia; vizir@opee.hcei.tsc.ru
* Correspondence: bakeeviyu@mail.ru

Abstract: We describe our investigations of a plasma-cathode electron source designed for the deposition of oxide coatings by the electron-beam evaporation of dielectric materials. Tests carried out using oxygen as the working gas showed that the source is operable without a change in parameters for at least ten hours of continuous operation. The current–voltage characteristics of the hollow-cathode plasma source in oxygen displayed a monotonically increasing character, and the voltage dependence of the discharge current was exponential. At the same time, for argon, nitrogen, and helium, the discharge voltage remained unchanged over a current ranging from 0.1 A to 1 A. A possible reason for these differences is the formation of oxides on the electrode surfaces for operation in the oxygen, impeding the discharge operation and requiring higher voltages for the same current as the other gases. The dependencies of the electron beam current on the accelerating voltage were monotonically increasing curves for all the gases except for helium, for which the beam current remained unchanged with increasing voltage over a range from two to ten kilovolts.

Keywords: electron beam; plasma source; plasma cathode; electron source characteristics; oxygen environment

1. Introduction

Particle-beam and plasma technologies are used in many applications for the modification of materials for various purposes, such as electron beam welding [1,2], plasma surface treatment [3–6], coating synthesis [7,8], etc. The electron beam evaporation of oxide targets is a promising method for the deposition of coatings with different functional properties [9]. A principal advantage of evaporation over ion sputtering is the faster deposition rate, which reduces the processing time. Since oxide materials are, as a rule, dielectrics, the accumulation of negative charge on the dielectric target is inevitable, which can cause the deflection and deceleration of the electron beam [10]. Another problem is the dissociation of oxides during evaporation, as a result of which the chemical composition of the deposited film differs from that of the target due to oxygen deficiency [11]. Both of these problems can be solved by using a fore-vacuum-pressure, plasma-cathode electron source [12], in which the electron beam is formed from electron emission from a gas discharge plasma at operating pressures in the range of 1–50 Pa. Under these conditions, plasma is formed along the electron beam trajectory (the "beam-plasma"), from which positive ions ensure the neutralization of the negative charge brought to the dielectric target by the electron beam. The problem of oxygen deficiency in the deposition can be avoided by carrying out the evaporation process in oxygen or an oxygen-containing environment. At the same time, despite the fact that plasma electron sources do not contain heated electrodes, the degradation of the electrodes under the action of oxygen plasma and, as a result, changes in the source characteristics cannot be ruled out. The purpose of the work described here was

to investigate the performance and characteristics of a plasma electron source in oxygen in comparison with its behavior in other gaseous media.

2. Materials and Methods

The experiment was carried out using a fore-vacuum-pressure, plasma-cathode electron source utilizing a hollow cathode discharge. The main elements of the source and a photograph are shown in Figure 1a,b.


(**a**)   (**b**)
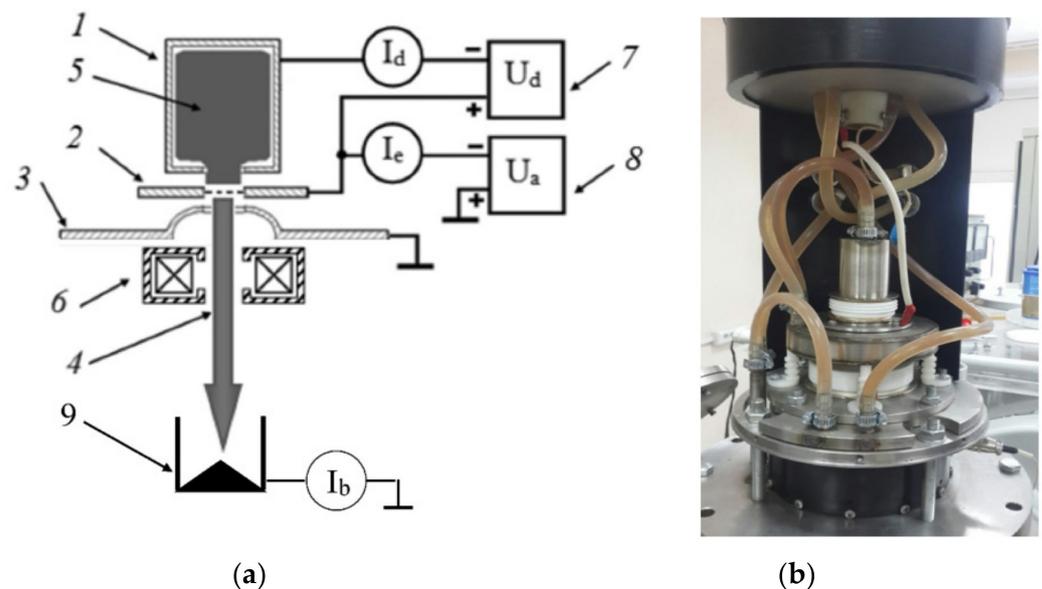
Figure 1. (**a**) Electrode circuit, and (**b**) photograph of the fore-vacuum plasma electron source: 1—water-cooled hollow cathode, 2—anode with emission grid, 3—accelerating electrode (extractor), 4—cylindrical electron beam, 5—emission plasma, 6—focusing system, 7—discharge power source, 8—accelerating voltage source, 9—collector.

A discharge with a hollow cathode 1 made of stainless steel with a diameter of 30 mm and a length of 80 mm was used in the source as the emission plasma generator. Anode 2 contained an emission window covered with a tantalum grid with 120 emission holes with a diameter of 0.7 mm. Holes were evenly distributed over the emission electrode over an area with a diameter of 13 mm. Beam accelerating voltage U_a was applied across the gap between anode 2 and accelerating electrode 3, located at a distance of 10 mm from the emission electrode. The hole in the extractor for propagation of the electron beam had a diameter of 15 mm. Electron beam 4 was focused by magnetic lens 6 and was terminated at collector 9 (Faraday cup), which served to measure beam current I_b. For the purposes of this study, the source was upgraded with thicker tantalum emission grids compared to those described in [3]. This made it possible to somewhat reduce the thermal load on the emission electrode by improving heat removal. The discharge and emission characteristics of the source were measured using four gases: argon, nitrogen, helium, and oxygen. After the vacuum chamber was evacuated to a pressure of 1 Pa, the working gas was admitted. The discharge was then ignited by application of voltage U_d, and the electron beam was formed upon increase in accelerating voltage U_a. Gas pressure p, current I_d, and voltage U_d of the discharge, as well as the accelerating voltage U_a and current I_b of the beam, were monitored. Gas pressure p was measured by a thermocouple vacuum gauge. The discharge voltage U_d, accelerating voltage U_a, and discharge current I_d were measured according to the electrical circuit shown in Figure 1a. Among these measured parameters, the beam current I_b had the maximum systematic error due to the formation of beam plasma in the area of its transportation. Thus, the collector current, identified as the beam current I_b, was distorted by the fraction of the current of the beam plasma particles to the collector.

The estimated error in the measurement of the beam current values due to this factor is presented in experimental graphs in the next section.

3. Results and Discussion

Figure 2 shows the current–voltage characteristics (CVC) of the hollow cathode discharge, which served as a plasma generator in the electron source. In Figure 2, 4–6 curves drawn through the experimental data points were obtained by spline interpolation. The resulting form of the current–voltage characteristic (Figure 2) is similar to the glow discharge used in discharge-emission systems with various configurations [13–15]: the discharge voltage increases with increasing current, and voltage saturation is observed. For nitrogen, argon, and helium as the working gases, the CVC became almost horizontal when the discharge current exceeded 100 mA. A different behavior was observed for oxygen—the voltage increased monotonically with the increasing current. Moreover, the dependence of the current on the voltage had an exponential character (Figure 3), which was confirmed by a linear approximation of the dependencies on the graph at coordinates $\ln I_d$, U_d. This different kind of characteristic can be explained as follows. For the argon, nitrogen, and helium, a normal glow discharge regime was produced, characterized by the invariance of the voltage with the increasing current. When applied to a discharge with a hollow cathode, this may mean gradual filling of the cathode cavity with plasma. A different behavior in the case of oxygen can be considered as an anomalous glow discharge, in which an increase in voltage is required to increase the current, so that each electron ejected from the cathode wall due to ion-electron emission can produce a greater number of ionization events, thereby increasing the plasma density. Moreover, at least a part of these ionization events was carried out in the sheath, due to which these electrons had time to gain sufficient energy for ionization. In other words, the conditions for avalanche electron multiplication were created. The fact that the discharge voltages in the oxygen noticeably exceeded the analogous values of the other gases was apparently due to the formation of oxides on the electrode surfaces. In turn, the higher voltages meant a greater sheath thickness between the plasma and the cathode wall, which ensured ionization in the sheath.


(a)

(b)
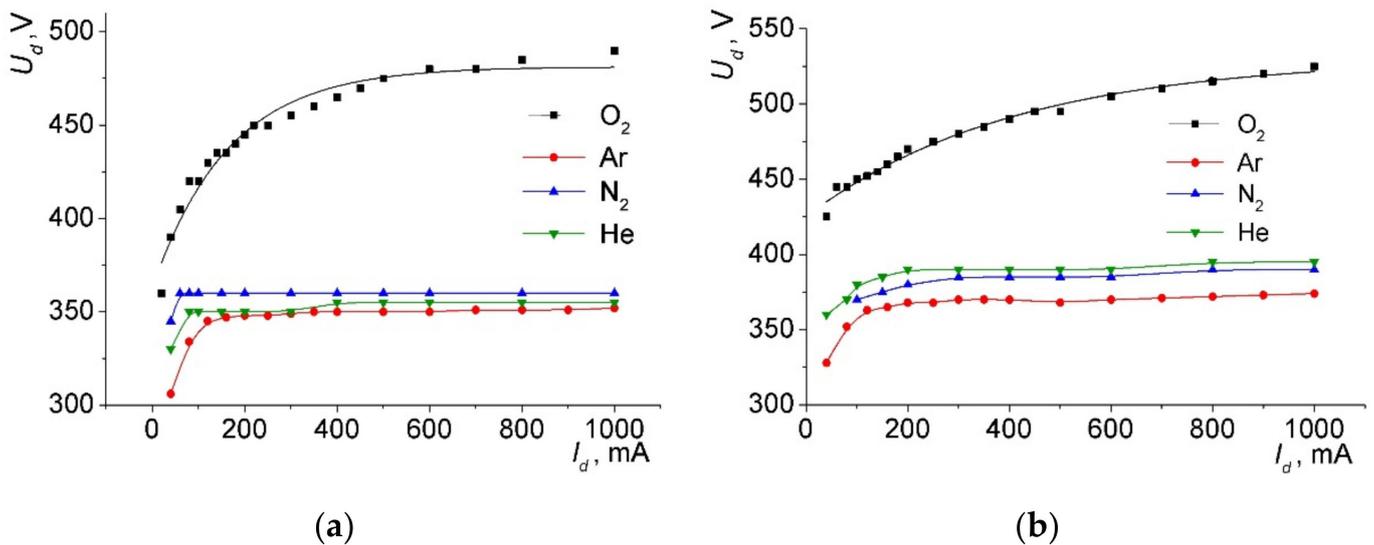
Figure 2. Characteristics of the discharge in oxygen, argon, nitrogen, and helium at various pressures: (**a**) 4.2 Pa and (**b**) 2 Pa.

The dependencies of the beam current on the accelerating voltage are shown in Figure 4. As can be seen, growing characteristics were observed for the oxygen, argon, and nitrogen, and the characteristics for the oxygen and argon had the greatest slope. The slope of the characteristics decreased with the decreasing gas pressure (Figure 4b). For the helium, the beam current remained unchanged over the entire range of the accelerating voltage. At

the same discharge currents and at accelerating voltages above 7 kV, for greater pressure (Figure 4a), the electron beam current increased in the following order: He, O_2, N_2, Ar. Figure 5 shows the dependence of the beam current I_b on the accelerating voltage U_a for various discharge currents I_d in oxygen. All the curves have the same form, which may indicate the same mechanism for the increase in I_b with increasing U_a. The dependencies of the beam current I_b on the discharge current I_d were close to linear (Figure 6). The relationship between the beam currents was the same as in Figure 4. The largest currents were observed for the argon, and the smallest for the helium.
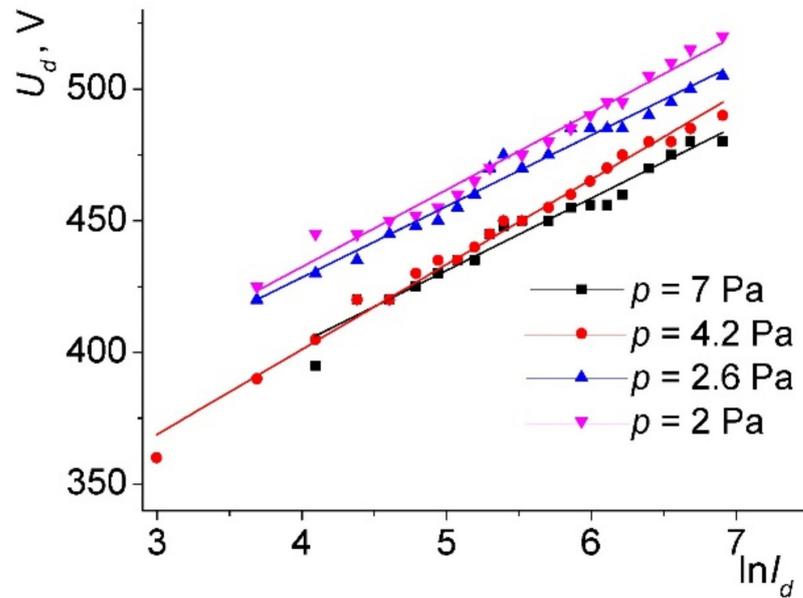

Figure 3. Current–voltage characteristic of the discharge in oxygen at semi-logarithmic coordinates for different pressures.
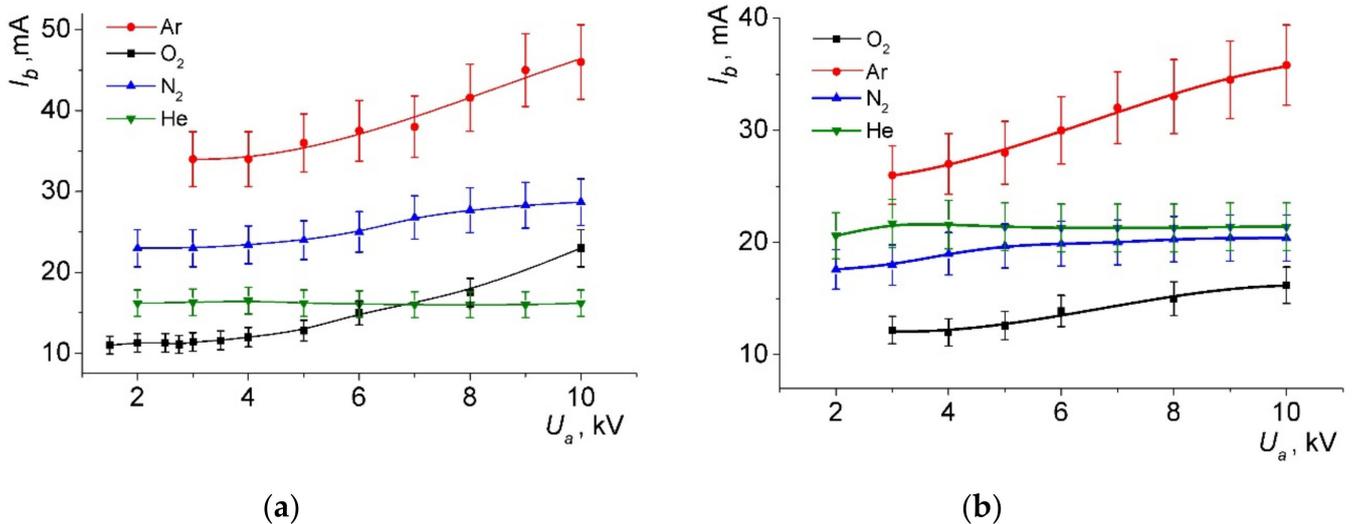
Figure 4. Beam current versus accelerating voltage for different pressures: (**a**) 4.2 Pa and (**b**) 2.6 Pa. Discharge current is 600 mA.
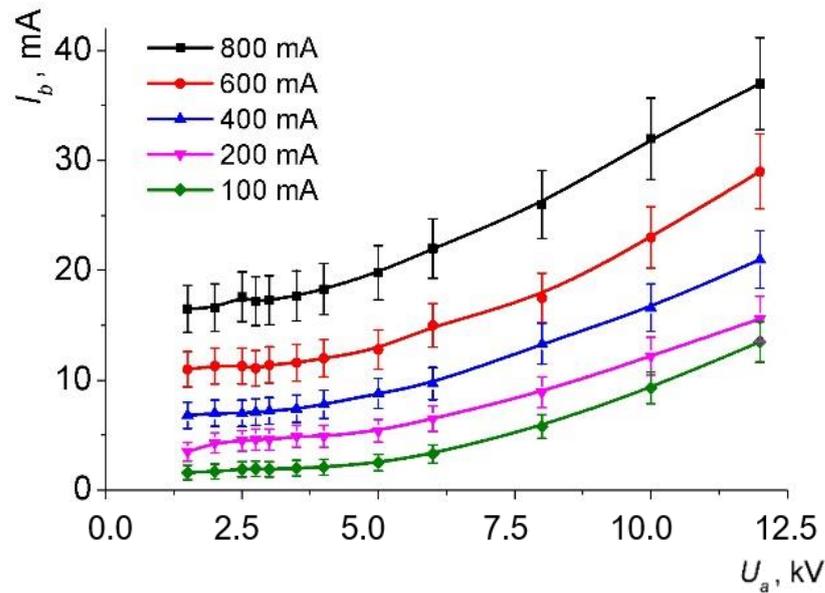
Figure 5. Beam current versus accelerating voltage for different discharge currents I_d. Oxygen pressure is 2.6 Pa.

(**a**) (**b**)
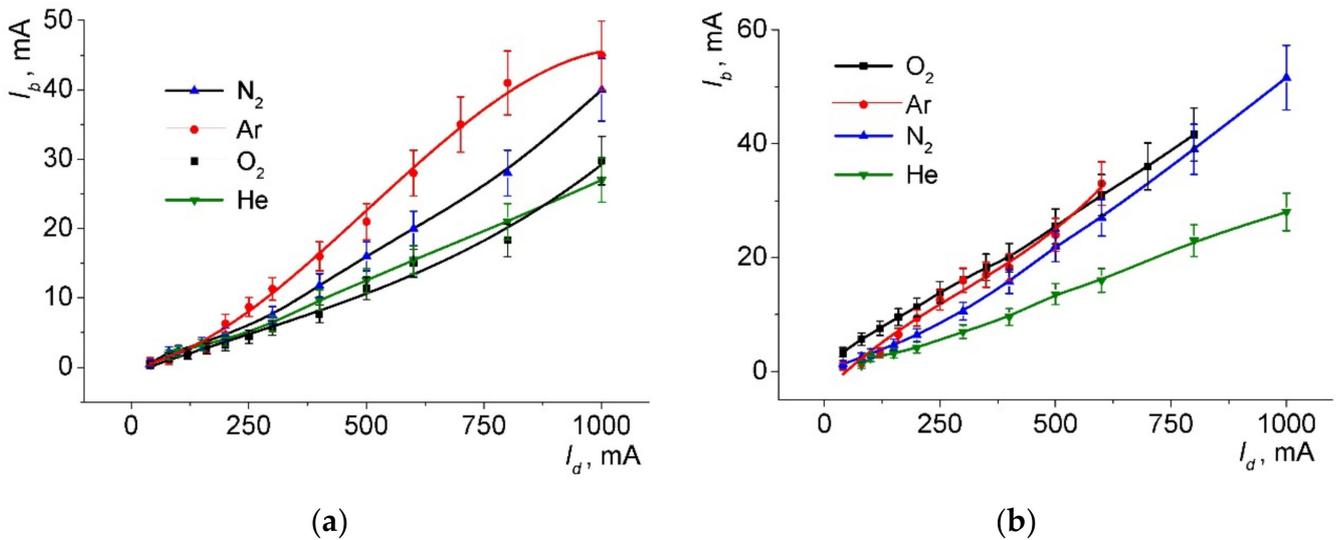
Figure 6. Beam current as a function of discharge current for various pressures: (**a**) 2.6 Pa and (**b**) 4.2 Pa. Accelerating voltage is 8 kV.

It should be noted that the effect of an increase in emissions and in the beam current from the accelerating voltage is typical for plasma sources during emission from the plasma at elevated pressures of the working gas only (above units of pascals) [16]. For plasma sources operating at pressures of 0.01–0.1 Pa, the entire increase in the emission current occurs only in the initial part of the dependence at voltages not exceeding a few kilovolts [15,17]. Only when particles are emitted from the plasma through a single emission hole [13,17] can the growing section stretch up to ten kilovolts; however, in any case, the degree of increase in the emission current decreases with increasing accelerating voltage. At the same time, it can be seen from the results obtained in Figures 4 and 5 that at elevated pressures, the slope of the dependence I_b (U_a) does not decrease with increasing accelerating voltage, but may even increase in some cases.

The indicated differences in the emission conditions can be explained by taking into account the presence of gas both in the beam propagation region and in the accelerating gap. Some conclusions can be drawn from a comparison of the ionization cross-sections for the

gases used. According to [18], for electron energies in the range of 1–10 keV, the ionization cross-sections decrease in the following order: Ar, N_2, O_2, He. Taking this into account, we can conclude that at a pressure of 4.2 Pa, the ratio between the beam currents for different gases can be due to both gas ionization in the accelerating gap and secondary electron emission from the tantalum grid under the action of ions emitted from the beam plasma and accelerated in the extractor-anode gap. An increase in beam current with increasing discharge current is quite expected, since the discharge current is directly related to the density of the emission plasma, and the current density j of the emission from the open plasma boundary is described by the well-known relation $j = env/4$, where v is the average thermal velocity of plasma electrons.

4. Conclusions

The primary result of our investigations is the experimental demonstration of the operability of a fore-vacuum-pressure, plasma-cathode electron source in an oxygen environment. The most noticeable effect of oxygen was manifested in the hollow cathode discharge used to generate the emission plasma. This effect expressed itself in an increase in the discharge voltage of about a hundred volts compared to the discharges in argon, nitrogen, and helium. Another difference lies in the growth in the voltage's dependence on the discharge current. The most probable reason for these differences is the oxidation of the discharge gap electrodes, which hinders the passage of current and causes increases in discharge voltage.

Author Contributions: Setting research objectives, V.B. and E.O.; technical preparation and experiments, K.K. and L.N.A.K.; systematization and analysis of results, V.B., I.B. and A.V.; writing the article, V.B., I.B. and E.O.; project administration, V.B. All authors have read and agreed to the published version of the manuscript.

Data Availability Statement: The data presented in this study are available on request from the corresponding author.

Conflicts of Interest: The authors declare no conflict of interest.

References

1. Węglowski, M.S.; Błacha, S.; Phillips, A. Electron beam welding–techniques and trends–review. *Vacuum* **2016**, *130*, 72–92. [CrossRef]
2. Sun, Z.; Karppi, R. The application of electron beam welding for the joining of dissimilar metals: An overview. *J. Mater. Processing Technol.* **1996**, *59*, 257–267. [CrossRef]
3. Abraha, P.; Yoshikawa, Y.; Katayama, Y. Surface modification of steel surfaces by electron beam excited plasma processing. *Vacuum* **2008**, *83*, 497–500. [CrossRef]
4. Lock, E.H.; Petrovykh, D.Y.; Mack, P.; Carney, T.; White, R.G.; Walton, S.G.; Fernsler, R.F. Surface composition, chemistry, and structure of polystyrene modified by electron-beam-generated plasma. *Langmuir* **2010**, *26*, 8857–8868. [CrossRef] [PubMed]
5. Shustin, E.G.; Isaev, N.V.; Temiryazeva, M.P.; Fedorov, Y.V. Beam plasma discharge at low magnetic field as plasma source for plasma processing reactor. *Vacuum* **2009**, *83*, 1350–1354. [CrossRef]
6. Jin, Q.Y.; Liu, Y.G.; Zhou, Y.; Wu, Q.; Zhai, Y.J.; Sun, L.T. RF and microwave ion sources study at institute of modern physics. *Plasma* **2021**, *4*, 332–344. [CrossRef]
7. Tanuševski, A.; Poelman, D. Optical and photoconductive properties of SnS thin films prepared by electron beam evaporation. *Sol. Energy Mater. Sol. Cells* **2003**, *80*, 297–303. [CrossRef]
8. George, J.; Menon, C.S. Electrical and optical properties of electron beam evaporated ITO thin films. *Surf. Coat. Technol.* **2000**, *132*, 45–48. [CrossRef]
9. Yushkov, Y.G.; Oks, E.M.; Tyunkov, A.V.; Yushenko, A.Y.; Zolotukhin, D.B. Electron-Beam Deposition of Aluminum Nitride and Oxide Ceramic Coatings for Microelectronic Devices. *Coatings* **2021**, *11*, 645. [CrossRef]
10. Vallayer, B.; Blaise, G.; Treheux, D. Space charge measurement in a dielectric material after irradiation with a 30 kV electron beam: Application to single-crystals oxide trapping properties. *Rev. Sci. Instrum.* **1999**, *70*, 3102–3112. [CrossRef]
11. Hoffman, D.; Leibowitz, D. Al_2O_3 films prepared by electron-beam evaporation of hot-pressed Al_2O_3 in oxygen ambient. *J. Vac. Sci. Technol.* **1971**, *8*, 107–111. [CrossRef]

12. Burdovitsin, V.A.; Zhirkov, I.S.; Oks, E.M.; Osipov, I.V.; Fedorov, M.V. A plasma-cathode electron source for focused-beam generation in the fore-pump pressure range. *Instrum. Exp. Tech.* **2005**, *48*, 761–763. [CrossRef]
13. Osipov, I.; Rempe, N. A plasma–cathode electron source designed for industrial use. *Rev. Sci. Instrum.* **2000**, *71*, 1638–1641. [CrossRef]
14. Semenov, A.P. Characteristics of a reflex discharge with a box-shaped cathode cavity and emission properties of the discharge plasma. *Tech. Phys.* **2007**, *52*, 276–280. [CrossRef]
15. Gavrilov, N.V.; Kamenetskikh, A.S. Glow-discharge-driven bucket ion source. *Rev. Sci. Instrum.* **2004**, *75*, 1875–1877. [CrossRef]
16. Burdovitsin, V.A.; Oks, E.M. Fore-vacuum plasma-cathode electron sources. *Laser Part. Beams* **2008**, *26*, 619–635. [CrossRef]
17. Grusdev, V.A.; Zalesski, V.G.; Antonovich, D.A.; Golubev, Y.P. Universal plasma electron source. *Vacuum* **2005**, *77*, 399–405. [CrossRef]
18. Raizer, Y.P. *Gas Discharge Physics*; Springer: Berlin, Germany, 1991.